



## Numerical and Experimental Investigation of Heat Transfer Enhancement by Hybrid Nanofluid and Twisted Tape

Noor F. A. Hamza, Sattar Aljabair 

Mechanical Engineering Dept., University of Technology-Iraq, Alsina'a street, 10066 Baghdad, Iraq.

\*Corresponding author Email: [me.19.06@grad.uotechnology.edu.iq](mailto:me.19.06@grad.uotechnology.edu.iq)

### HIGHLIGHTS

- Hybrid nanofluid in a tube with a typical inserted twisted tape has been investigated experimentally and numerically.
- The most important basic dimensionless parameters, including Reynolds number, Nusselt number, and Friction factor, have been studied.
- The results proved that there is a noticeable improvement in heat transfer in the presence of a typical inserted twisted tape.

### ABSTRACT

This paper presents an experimental and numerical study to investigate the heat transfer enhancement in a horizontal circular tube using hybrid nanofluid (CuO, Al<sub>2</sub>O<sub>3</sub>/ distilled water) and fitted with twisted tape (typical twisted tape, with twist ratios (TR=9.2). Under fully developed turbulent flow and uniform heat flux conditions, the studied hybrid nanofluid concentrations are (=0.6, 1.22, and 1.8% by volume). The experimental test rig includes all the required instruments to study the heat transfer enhancement. All the tests were carried out with a Reynolds number range of 3560-8320 and uniform heat flux (13217.5 W/m<sup>2</sup>. The twisted tape, manufactured from polylactic acid (PLA) by 3-dimensional printer technology, was inserted inside the tube. In this numerical study, the finite volume method (CFD) procedure was employed to pattern the forced convection turbulent flow through the tube. For hybrid nanofluid with twisted, the maximum enhancement in the maximum thermal performance factor was 2.18 for  $\phi = 1.8\%$ , while for a tube (water with twisted) under the same conditions, it was (2.04). A high Nusselt number was obtained with a concentration of 1.8% and an enhancement in the heat transfer of about 6.70% than water.

### ARTICLE INFO

**Handling editor:** Ayad M. M. Jubori

#### Keywords:

Hybrid nanofluid; Turbulent flow; CFD; Heat transfer; Typical twisted tape; Thermal performance factor

### 1. Introduction

Many scientists have been interested in improving the shape of pipes and thus increasing the performance coefficient of enormous heat exchangers that contain many smooth tubes due to the urgent need to improve their condition. Adding a twisted tape inside pipes is one of the most well-known and extensively utilized strategies for increasing the heat exchanger efficiency in recent research. Smithberg and Landis [1] were the first scientists who applied twisted tape to the tube and investigated its impact on the heat transfer coefficient and pressure drop inside the pipe in 1964. Researchers such as Hong and Bergles [2] and Manglik and Bergles [3] followed up on their twisted tape studies in 1976 and 1993, respectively, and all agreed that the presence of twisted tape improved heat transfer. As a result of the global energy shortage problem, this is one of the most important concerns due to the considerable and ongoing increase in demand, the growing scarcity of energy supplies, and the high cost of production. The researchers are working to improve the performance of thermal systems, minimize their size, and reduce energy consumption rates. The heat transfer coefficient and pressure drop are two of the most important parameters impacting the growth of any thermal system. The thermal resistance of the boundary layer must be minimized, and the turbulence in the fluid flow must be enhanced to achieve the best heat transfer coefficient. Due to the compact structural design, which accelerates the heat transfer process, the tube with twisted tape technology is one of the essential technologies utilized in industries and energy sectors. Nanofluid is a new class of heat transfer fluids, and nanoparticles can also be mixed with the base fluid, which enhances the base fluid's thermal properties. The research trend is significantly changing towards

nano fluids applications in the heat transfer systems due to limitations on future development in the thermos-physical characteristics of traditional working fluids [4]. The term "nanofluid" refers to a mixture of metallic and nonmetallic nanoparticles distributed in water, oils, and other base fluids [5]. Choi [6] created the term nanofluid in 1995, describing a fixed solution of a limited number of extremely tiny particles ranging from 1 nm to 100 nm. These particles boosted the thermal conductivity of the base fluid, raising the heat transfer coefficient. Numerous studies were reported on the heat transfer applications of nanofluids in thermal systems such as tubes. The heat transfer using conventional fluids (water, oil, and ethylene glycol) were mainly applied in machine tools with a large variety of devices. The number of dispersed particles, material type, particle shape, volume percentage, and other factors influences heat transfer enhancement's efficacy. The fundamental goal of creating hybrid nanofluids is to learn about the characteristics of the components that make them up. A single material may or may not have all of the desirable attributes necessary for a certain application; it may have excellent thermal or rheological capabilities. However, in many practical applications, a trade-off between numerous features is necessary, which is where the usage of hybrid nanofluid comes in [7]. Hybrid nanofluid is the new generation of the heat transfer fluid for various heat transfer applications where the transport characteristics are substantially higher than the base liquid. Furthermore, due to the synergistic effect, the hybrid nanofluid is projected to have greater thermal conductivity than separate nanofluids. The hybrid nanofluid convective heat transfer two-phase mixture model was used by Labib et al. [8]. They used two distinct base fluids to look at the thermal impact of liquids transmission while combining alumina nanoparticles. The use of ethylene glycol as a base fluid increased the heat transfer better than water, according to the findings. The computational model for CNTs/water nanofluid was compared to the literature to ensure that it was accurate. Bbasi [9] explored the heat transfer of hybrid nano-fluids moving through a circular tube during a turbulent flow. The Fe<sub>3</sub>O<sub>4</sub>/MWCNT Nano composites were made in-situ using a process that comprised dispersing carboxylate carbon nanotubes in water and combining ferrous and ferric chlorides. Compared to base fluid data, for a particle loading of 0.3% at a Reynolds number of 22000, the heat transfer augmentation was 31.10%, with a penalty of 1.18 times greater pumping power. The input and output parameter correlation equations were provided, and they agreed well with the experimental results. The nanofluid was created by suspending titanium/copper nanoparticles in water with a volume fraction from 0.1% to 1.0%. The Nusselt number values increased by 48.4% up to 0.7% the concentration of hybrid nanofluid, according to the findings [10]. The effect of functionalization on the stability and thermal conductivity (k) of a CNT-Al<sub>2</sub>O<sub>3</sub> hybrid nanofluid was investigated. The heat transfer of turbulent nanofluids in the presence of a magnetic field was studied in [11]. It was found that the Nusselt number increased in a linear relationship with Reynolds number, nanoparticle volume percentage, and turbulent Eckert number. At the same time, it decreased in an inverse relationship with the Hartmann number and turbulence parameter, according to the findings. The work on hybrid nanofluids is very limited, and many experimental studies are still being done.

Maddah et al. [12] investigated a twin tube heat exchanger and examined the effect of a twisted-tape tabulator and nanofluid on the heat transfer. A titanium dioxide nanofluid was used to investigate the heat transfer in a twin pipe H.E and twisted-tape components in an experimental setting. The heat exchanger's working fluid was water, and the smaller pipe's outer and inner diameters were 16 and 8 mm, respectively. Twisted tapes with a length of 120 cm, a width of 5 mm, and a thickness of 1 mm were made from aluminum sheets. At a volume concentration of 0.01%, titanium dioxide nanoparticles with a diameter of 30 nm were created. They looked at countercurrent flow, turbulent flow regimes, heat transfer changes, heat transfer coefficient, and its impact on nanoparticle concentration, mass flow rate, and temperature impacts. The heat transfer coefficient improved by (10% - 25%) when the nanofluid and twisted tape were used.

Furthermore, while utilizing a twisted tape with 0.01% TiO<sub>2</sub>/water nanofluid, when employing just 0.01% TiO<sub>2</sub>/water nanofluid, the pressure loss and friction factor were found to be greater. Empirical correlations were used to validate the data from the experimental findings [13]. Several twisted tape inserts and TiO<sub>2</sub>/water nano-fluid were used to improve the heat transfer. Because of the continuous multiple swirling flow and multi-longitudinal vortices flow along the test tube, the pipe inserted with multiple twisted tapes had a greater thermal performance factor than the plain pipe inserted with a single twisted tape. Because of the increased contact surface area, residence time, swirl strength, and fluid mixing with multi-longitudinal vortex flow, the increased number of twisted tape inserts resulted in enhanced thermal performance.

Furthermore, in reality, twisted tapes used in co-current have shown to be superior energy-saving systems, particularly at low Reynolds numbers. This was notably true in cross directions for quadruple counter tapes (CC-QTs), which provided an excellent heat transfer with a minimal friction loss penalty. The maximum thermal performance factor was achieved with the usage of CC-QTs, which was 1.45. Compared to pure water, utilizing water containing TiO<sub>2</sub> nanoparticles as a working fluid resulted in better thermal performance. When compared to the simple pipe and water as a working fluid, the heat transfer and the friction factor rose to 3.52 and 11.7 times, respectively, in the pipe inserted CC-QTs with TiO<sub>2</sub>+water nanofluid at  $\Phi=0.21\%$  by volume.

In the present study, single-phase techniques consider nanoparticles and base fluid as a single homogenous fluid. First, the effects due to the varying volume concentrations of Al<sub>2</sub>O<sub>3</sub>/CuO hybrid nanoparticles on the thermophysical properties (thermal conductivity, viscosity, and density) of Al<sub>2</sub>O<sub>3</sub>/CuO/ water-based nanofluids with a typical twisted tape have been investigated. Then, how twisted tapes improve the thermal performance factor of a heat exchanger tube by reducing the friction factor and increasing P.E.C (thermal performance factor) has been reported.

## 2. Methodology

The heat transfer and fluid movement into the heat pipe is a complicated procedure. As a result, a thermal CFD simulation's efficiency is influenced by various parameters. The creation of the model geometries and their integration in a physical domain, grid generation, and the selection of an appropriate numerical computing technique are all important

elements that might influence the simulation process' success. Turbulent flow experiments and numerical were carried out on a smooth tube (tube without twisted tape) with a hybrid nanofluid, and the results were compared to the Duttis -Bolter equation. In the next lines, the main steps of the studies are briefly discussed

### 3. Experimental Procedure

#### 3.1 Test Rig

The experimental test was designed for convective heat transfer in a turbulent flow regime. The horizontal test section was a copper tube with a 0.02 m (3/4") diameter and a 2 m length. It is heated by an electrical coil constructed of tungsten material and eight meters long with (2000 W) heating power. Heat flux is generated by connecting the tube to an AC power supply. The tube has a fully developed hydro-dynamic length of (1.5 m). Insulation of the rock wool type was used to insulate the test section. The temperatures along the outside surface of the tube at the heated test section were measured using three thermocouples (K-type), each separated by 50 cm. The entrance and exit temperatures of the fluid in the test portion were measured using two thermocouples submerged in the flow. All thermocouples were linked to an Arduino system, which was used to record and display the thermocouple readings on a personal computer. A flow meter was used to measure the flow rate range (0–20 l/min). The pressure loss over the (2 m) length of the test portion was measured using two pressure gauges. Photo of the experimental test rig is shown in Figure (1), and table (1-1) includes the equipment, its operation ranges, and its systematic error.

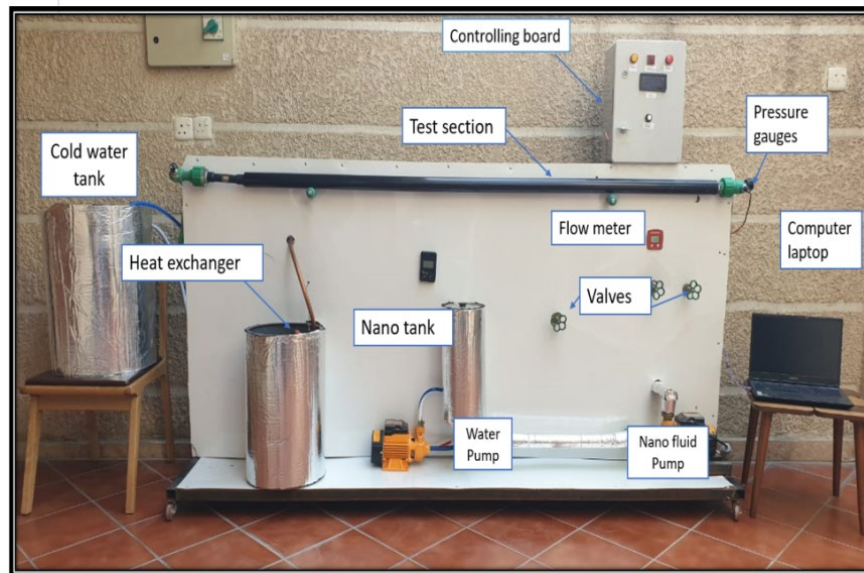


Figure 1: Photo of the test rig

Table 1: The equipment its operation ranges

Equipment	Operation range	Uncertainty
Flow meter	(0-30)	±0.1
Thermocouples	(0-180°C)	± 1
Ammeter	(0-25)	±0.1
Voltmeter	ampere (0-220)volte	±0.1

#### 3.2 Properties of Hybrid Nanofluids

The CuO + Al<sub>2</sub>O<sub>3</sub> nanoparticles suspended in water nanofluids under investigation were regarded as a single-phase stream, a Newtonian fluid that is highly viscous, and an isotropic fluid. The effective thermal properties density ( $\rho_{nf}$ ), specific heat capacity ( $Cp_{nf}$ ), thermal conductivity ( $k_{nf}$ ) and viscosity ( $\mu_{nf}$ ) of the hybrid nanofluids were evaluated using classical formulas developed [14, 15].

The volume fraction of nanoparticles in the nanofluid:

$$\Phi_{\text{hybrid nanofluid}} = \Phi_{\text{nanoparticle1}} + \Phi_{\text{nanoparticle2}} \tag{1}$$

The density of hybrid nanofluid:

$$\rho_{hnf} = \rho_{np1}\Phi_{np1} + \rho_{np2}\Phi_{np2} + (1 - \Phi_{hnf})\rho_{bf} \tag{2}$$

Specific heat of hybrid nanofluid:

$$Cp_{hnf} = \frac{\Phi_{np1}\rho_{np1}Cp_{np1} + \Phi_{np2}\rho_{np2}Cp_{np2} + (1 - \Phi_{hnf})\rho_{bf}Cp_{bf}}{\rho_{hnf}} \tag{3}$$

The viscosity of hybrid nanofluid:

$$\mu_{hnf} = \frac{\mu_{bf}}{(1 - \Phi_{np1} - \Phi_{np2})^{2.5}} \tag{4}$$

Thermal conductivity of hybrid nanofluid:

$$K_{hnf} = K_{bf} \frac{(\frac{\Phi_{p1}k_{p1} + \Phi_{p2}k_{p2}}{\Phi_{total}}) + 2k_{bf} + 2(\Phi_{p1}k_{p1} + \Phi_{p2}k_{p2}) - 2\Phi_{total}k_{bf}}{(\frac{\Phi_{p1}k_{p1} + \Phi_{p2}k_{p2}}{\Phi_{total}}) + 2k_{bf} - (\Phi_{p1}k_{p1} + \Phi_{p2}k_{p2}) + \Phi_{total}k_{bf}} \tag{5}$$

Here,  $\Phi_{hnf}$  is the volume fraction of hybrid nanofluid,  $\Phi_{np1}$  is the volume fraction of nanoparticle1,  $\Phi_{np2}$  is the volume fraction of nanoparticle 2,  $\rho_{hnf}$  (kg/m<sup>3</sup>) is the density of hybrid nanofluid,  $\rho_{np1}$  (kg/m<sup>3</sup>) is the density of nanoparticle1,  $\rho_{np2}$  (kg/m<sup>3</sup>) is the density of nanoparticle 2,  $Cp_{hnf}$  (J/kg·K) is the specific heat of hybrid nanofluid,  $Cp_{np1}$  (J/kg·K) is the specific heat of nanoparticle1,  $Cp_{np2}$  (J/kg·K) is the specific heat of nanoparticle 2,  $K_{hnf}$  (W/m·K) is the thermal conductivity of hybrid nanofluid,  $K_{np1}$  (W/m·K) is the thermal conductivity of nanoparticle1,  $K_{np2}$  (W/m·K) is the thermal conductivity of nanoparticle 2, and  $\mu_{hnf}$  (Pa·s) is the viscosity of hybrid Nanofluid. The thermal properties of CuO and Al<sub>2</sub>O<sub>3</sub> Nanopowders and hybrid nanofluids are listed in Table 2 and 3, respectively.

**Table 2:** Thermal properties of the nanoparticles and base fluid [16, 17]

Properties	Water	Al <sub>2</sub> O <sub>3</sub>	CuO
ρ (Kg/m <sup>3</sup> )	997	3980	6400
Cp (J/kg·K)	4180	765	535.6
K (W/m·K)	0.607	40	76.5
μ (Pa·s)	0.000891	—	—

**Table 3:** Thermal properties of the hybrid nanofluid

Φ	ρ (Kg/m <sup>3</sup> )	Cp (J/kg·K)	K (W/m·K)	μ (Pa·s)
0.3%	1248.28	3293.619	0.88913	0.00104
0.6%	1499.56	2704.299	1.20773	0.00123
0.9%	1750.84	2284.136	1.57035	0.00146

### 3.3 Twisted Tape (Typical Type)

The twisted tapes were made by twisting a metal strip of finite length with various pitches and twist ratios. The pitch is the distance required for the strip to rotate 180, and the twist ratio (T.R) is the ratio of pitch to the width of the tape. The twisted typefaces were created using the Solid Works program (2020). The typical twisted tape (T.T) has been drawn and submitted to a 3D printer. In the production process, PLA (poly lactic acid) was used. The dimensions of the twisted tape used (0.018 m) width, twisted pitch (166.6), and thickness (1.5 mm) as shown in Figure (2a). The components were trimmed to a length of 50 cm and separated into four portions before being bonded together. The 3D printer is depicted in Figure (2b).

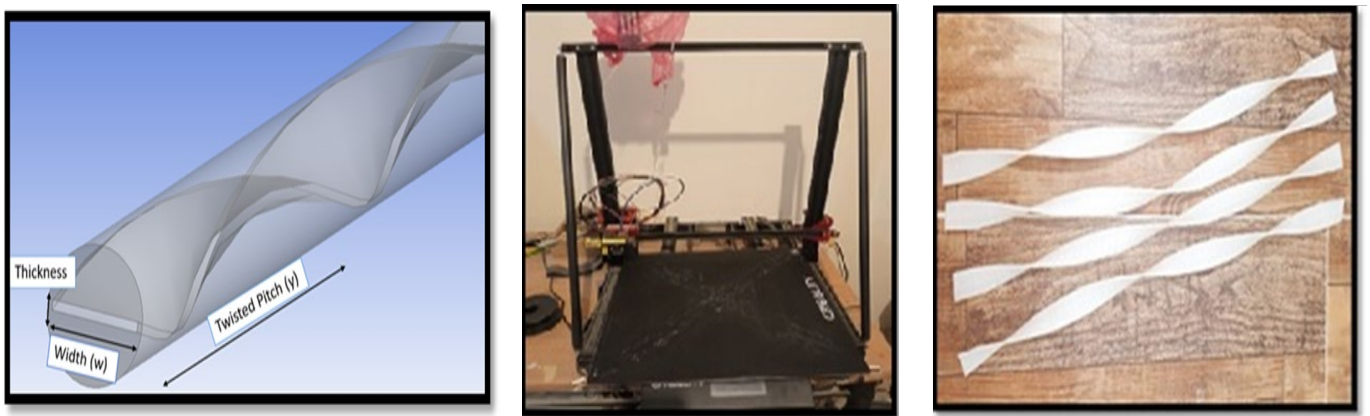


**Figure 2:** A. Twisted tape dimensions, B. The 3D Pinter and the manufactured twisted tape

### 3.4 Analysis of the Error (Uncertainty)

The quantities used to estimate the Nusselt number are subject to certain uncertainties due to errors in the measurement, and these particular uncertainties are presented. The analysis was carried out based on the suggestion by Robert J. Moffat [18], and the table below shows the instrument used its range and its error.

The result (R) is generally calculated from the data, Xi. Thus, one can write:

$$R = R(X_1, X_2, X_3 \dots \dots, X_i) \quad \delta R X_i = \frac{\partial R}{\partial X_i} * \delta X_i$$

$$\delta R = \left[ \sum_{i=1}^m \left( \frac{\partial R}{\partial X_i} * \delta X_i \right)^2 \right]^{0.5}$$

The uncertainty interval (S) in the result can be given as:

$$S_R = \left[ \left( \frac{\partial R}{\partial X_1} S_{X1} \right)^2 + \left( \frac{\partial R}{\partial X_2} S_{X2} \right)^2 + \dots \dots \dots + \left( \frac{\partial R}{\partial X_i} S_{Xi} \right)^2 \right]^{0.5} \tag{6}$$

In a dimensionless form:

$$\frac{S_R}{R} = \left[ (R_{X1} S_{X1})^2 + (R_{X2} S_{X2})^2 + \dots \dots \dots + (R_{Xi} S_{Xi})^2 \right]^{0.5},$$

where,  $R_{Xi} = \frac{\partial R}{\partial X_i}$

The Nusselt number (Nu):

$$Nu = \frac{h_i d_i}{k} = \frac{Q d_i}{A_s \Delta T_s K} = \frac{\dot{m} C_p \Delta T_b d_i}{A_s \Delta T_s K}$$

$$\Delta T_{bulk} = T_{out} - T_{in}, \quad \Delta T_s = T_{wall} - T_{bulk}, \quad A_s = \pi d_o L$$

The uncertainty Nusselt number is calculated by this equation:

$$S_{Nu} = \left[ \left( \frac{\partial Nu}{\partial \dot{m}} S_{\dot{m}} \right)^2 + \left( \frac{\partial Nu}{\partial \Delta T_b} S_{\Delta T_b} \right)^2 + \left( \frac{\partial Nu}{\partial \Delta T_s} S_{\Delta T_s} \right)^2 \right]^{0.5} \tag{7}$$

Relative error =  $\frac{S_{Nu}}{Nu}$

Sample of the values of Nusselt numbers and uncertainty are given in Tables (4) and (5)

**Table 4:** The calculated Nusselt numbers for water in smooth cases

Flow rate L/min	Nusselt number-water Error	Relative error
3	0.2038	0.0083
4	0.1606	0.00654
5	0.1491	0.00607
6	0.1698	0.0069
7	0.1644	0.0066

**Table 5:** The calculated Nusselt numbers for hybrid nanofluid for smooth case

Flow rate L/min	Nusselt number for hybrid nanofluid at $\Phi=0.6\%$	
	Error	Relative error
3	0.201	0.00818
4	0.1763	0.00718
5	0.1458	0.00593
6	0.1482	0.0063
7	0.1342	0.00546

Error: means the uncertainty Nusselt number in the above Equation (7)

## 4. Numerical Method

### 4.1 Simulation Method

In the current study, a 3-dimensional model design has been used for modeling the horizontal pipe and the typical twisted tape inserted. ANSYS Fluent 19.0 was used in modeling the present design to estimate the behavior of flow and heat transfer. In Figure (3), a design modeler was employed for building the computational domain, and the dimensions of the pipe are (2000

mm) in length and (22,20 mm) in outer and inner diameter, respectively. The next assumption is expressed for constructing the model

The fluid flow is turbulent, single-phase, incompressible, and steady-state condition. The turbulent flow across the tube and the twisted tape areas were computed using the finite volume CFD technique. To ensure the flow is hydro-dynamic and fully developed, entrance length should be added to the test section length. For turbulent flow, the entrance length is according to the equation below as [2]

$$\frac{Le}{D} = 4.4 Re^{1/6} \quad \text{for } 2300 < Re < 10,000 \quad (8)$$

$$Re = \frac{\rho u d}{\mu} \quad (9)$$

$\rho$  and  $\mu$  are the density and the dynamic viscosity of the fluid inside the tube, and  $u$  is the flow velocity.

Based on the above equations, the minimum hydro-dynamic entrance length is 0.344 m, while the maximum length is 0.396 m. Therefore, the entrance length was 0.5 m to ensure passing the entrance region. Navier-stokes equations, energy equations, and continuity equations were used to solve the flow distribution. The meshing was focused around the pipe wall and the twisted insert to ensure the anticipation of the temperature and velocity distribution. Figure (4) reveals the mesh generation for the test section in this instance. All the results were analyzed, and the conclusions and suggestions were written.

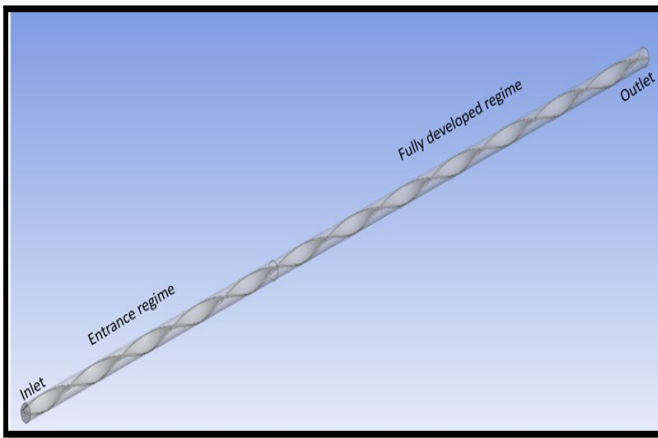


Figure 3: Geometry shape

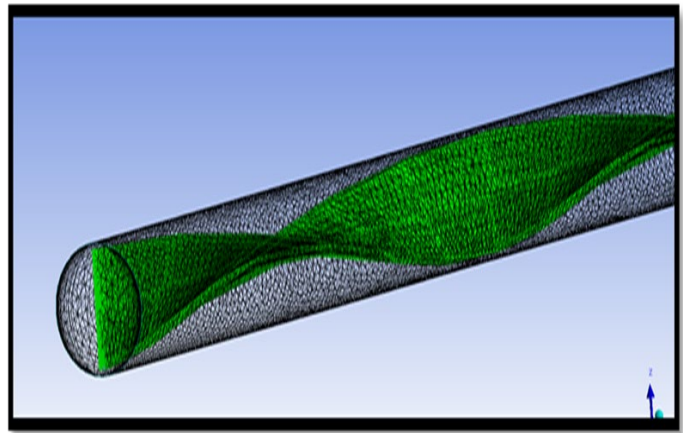


Figure 4: Mesh generation

### 4.2 Mesh Generation and Grid Independence

Grid Independence is the term used to designate the enhancement of results by using successively smaller cell sizes for the calculations. A calculation should reach the correct result, so the mesh becomes smaller; hence the term is known as grid Independence. The ordinary CFD technique is to start from coarse mesh and gradually improve it until the changes detected in the values are smaller than a pre-defined acceptable error. There are two problems with this. Firstly, it can be quite difficult with other CFD software to gain even in a single coarse mesh resulting in some problems. Secondly, refining a mesh by a factor of two or above can take more time. This is clearly offensive for software intended to be used as an engineering tool designed to operate to constricted production limits. In addition, the other issues have added significantly to the perception of CFD as an extremely difficult, time-consuming, and costly methodology. Finally, The Nusselt number was recorded and arranged in each case to achieve grid independence. The number of nodes and elements was (859625) and (1976913), respectively, with an error of about 0.754% in ANSYS-FLUENT. The gained results are tabulated in Table (6) and Figure (5).

Table 6: Grid Test Results.

Max. face size	Element no.	Node no.	$Nu_{ave}$
4	552202	25078	35.6931
3	784248	355993	36.9544
2	1976913	859625	37.2354
1	9107131	3656630	37.236

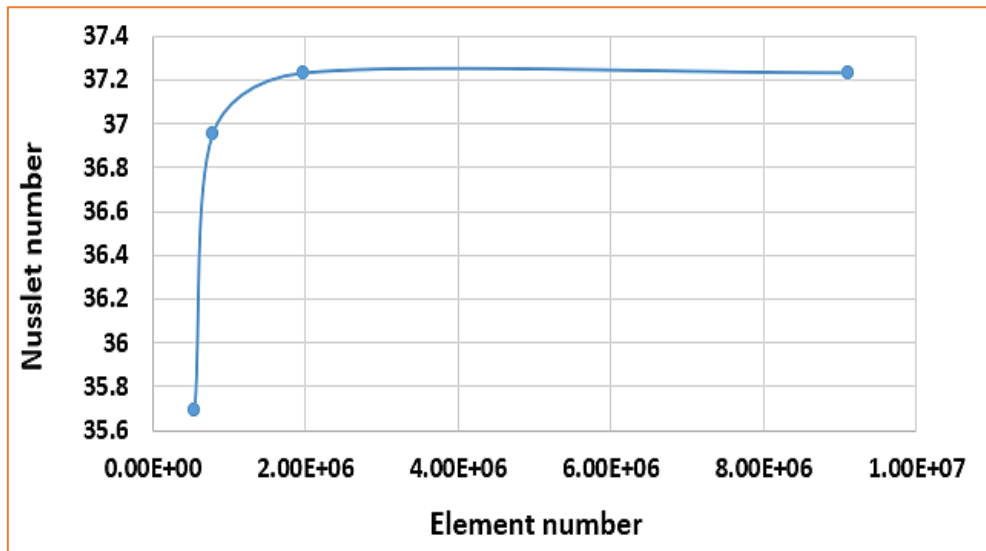


Figure 5: Grid independent test

### 4.3 Boundary Conditions

The volume fractions of the CuO + Al<sub>2</sub>O<sub>3</sub>/water hybrid nanofluid used as the input fluids are (0.3, 0.6, and 0.9%) with the inlet temperature of 25°C. Water and CFD simulations were performed using a uniform velocity profile at the entrance and a pressure outlet condition at the outlet zones for comparison. The perfectly smooth walls of the tube were assumed, and the Re was varied between 3560 - 8320 as input data at each iteration step.

### 4.4 Governing Equations

The governing equations to be solved are the continuity momentum and the equation of the energy [19].  
 Mass Conservation (Continuity):

$$\frac{\partial u}{\partial x} + \frac{\partial v}{\partial y} + \frac{\partial w}{\partial z} = 0 \tag{10}$$

Momentum Equation:

X- Momentum

$$\rho \left( u \frac{\partial u}{\partial x} + v \frac{\partial u}{\partial y} + w \frac{\partial u}{\partial z} \right) = \rho X - \frac{\partial P}{\partial x} + \frac{1}{3} \mu \frac{\partial}{\partial x} \left( \frac{\partial u}{\partial x} + \frac{\partial v}{\partial y} + \frac{\partial w}{\partial z} \right) + \mu \nabla^2 u \tag{11}$$

Y- Momentum

$$\rho \left( u \frac{\partial v}{\partial x} + v \frac{\partial v}{\partial y} + w \frac{\partial v}{\partial z} \right) = \rho Y - \frac{\partial P}{\partial y} + \frac{1}{3} \mu \frac{\partial}{\partial y} \left( \frac{\partial u}{\partial x} + \frac{\partial v}{\partial y} + \frac{\partial w}{\partial z} \right) + \mu \nabla^2 v \tag{12}$$

Z- Momentum

$$\rho \left( u \frac{\partial w}{\partial x} + v \frac{\partial w}{\partial y} + w \frac{\partial w}{\partial z} \right) = \rho Z - \frac{\partial P}{\partial z} + \frac{1}{3} \mu \frac{\partial}{\partial z} \left( \frac{\partial u}{\partial x} + \frac{\partial v}{\partial y} + \frac{\partial w}{\partial z} \right) + \mu \nabla^2 w \tag{13}$$

Energy Equation:

$$\rho C_p \left( u \frac{\partial T}{\partial x} + v \frac{\partial T}{\partial y} + w \frac{\partial T}{\partial z} \right) = \left( u \frac{\partial P}{\partial x} + v \frac{\partial P}{\partial y} + w \frac{\partial P}{\partial z} \right) + k_s \left( \frac{\partial^2 T}{\partial x^2} + \frac{\partial^2 T}{\partial y^2} + \frac{\partial^2 T}{\partial z^2} \right) \tag{14}$$

$u, \rho, \nu, T$  and  $P$  are the average velocity, density, kinematic viscosity, temperature, and pressure, respectively.

The turbulence ( $k - \epsilon$ ) model is economical with logical accuracy for a wide turbulent flow range, and it is generally used in heat transfer simulation.

### 4.5 Convergence Criteria

The CFD technique requires iterating the solution of the fluid flow equations till it is converged, as shown in Figure (6), exhibiting the convergence history for continuity, momentum, energy, and turbulence equations. The iterations are stopped when the solution remains the same within the accuracy of the selected convergence criteria. The most widely used method to check the solution convergence is the error residuals, which is the difference between the values of a variable in two consecutive iterations normalized by the largest absolute residual for the first five iterations. The solution is said to be converged when the residuals are below a tolerance limit of ( $10^{-6}$ ) for the all fluid flow equations presented above.

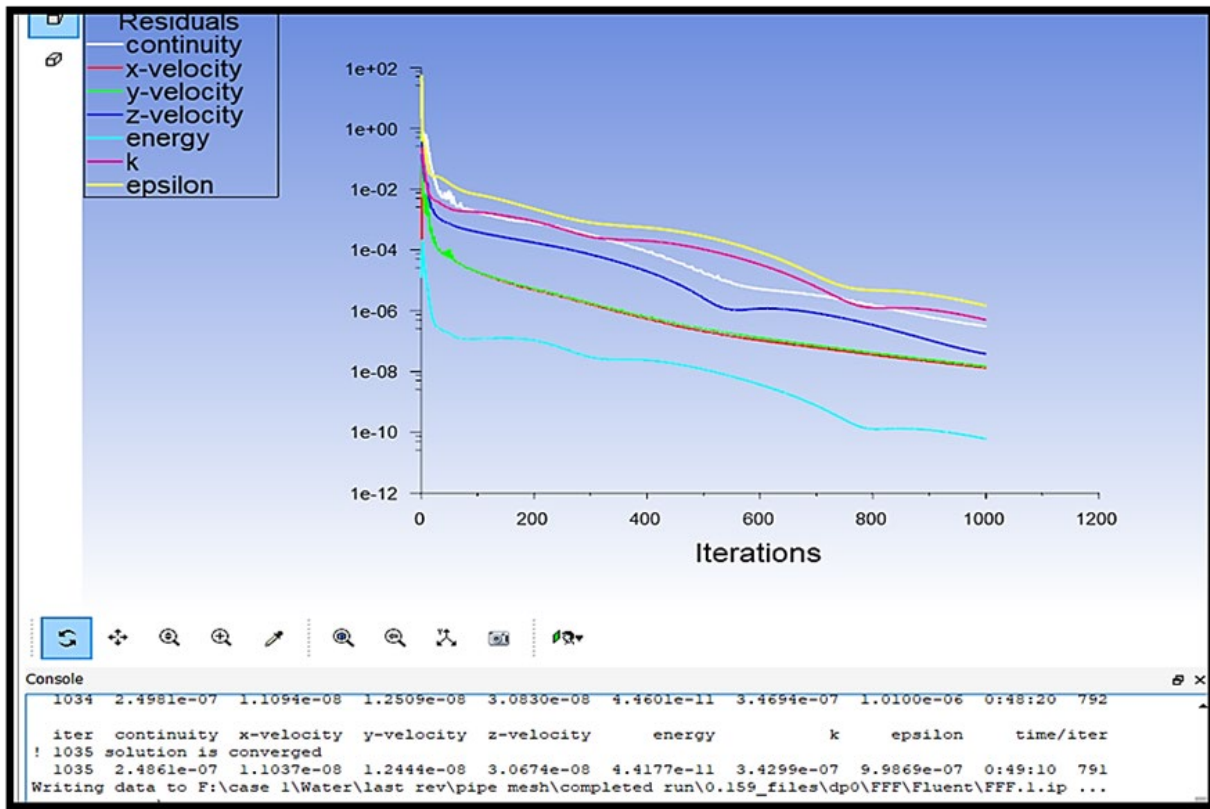


Figure 6: Iteration history of the numerical calculation

## 5. Results and Discussion

The measured temperature at the outlet, pressure and flow rates allowed for calculating the heat transfer rates, friction factor, heat effectiveness, thermal performance factor, and local Nu from the tube side of the turbulent flow. In addition, the effect of twisted tape was considered at different volume flow rates of hybrid nanofluid (3, 4, 5, 6, and 7 l/min). Therefore, in this section, numerical and experimental results have been presented and discussed.

### 5.1 Validation

To confirm the test facilities and the values gathered, the heat transfer and pressure loss of a simple tube (2 m) long as a test portion were investigated. For the current test, the Nusselt number vs. Reynolds number for a fully developed turbulence within a portion using pure water as the working fluid, as well as the well-known Dittus–Boelter equation is displayed in Figure (7a) [20].

$$Nu = 0.023 Re^{0.8} Pr^{0.3} \tag{15}$$

The present heat transfer data at the test facility correspond well with the aforementioned equation, with a maximum variation (4.638%)—the friction factor's agreement with the published data of Blasius eq. (16) is elucidated in Figure (7-b), with a maximum divergence of (5.122%).

$$Friction = 0.316 Re^{-0.25} \tag{16}$$

### 5.2 The Numerical Comparison Between the Straight Pipe and Twisted Tape Insert

Figure (8) manifests the (Nu) variation for both the straight pipe without twisted and water as working fluid and twisted tape inside the pipe and water for the volume flow rate range (3 - 7l/min). The Nu number during the plain pipe at the volume flow rate (3, 7 l/min) is (27.065, 56.053), respectively and for the pipe with twisted 37.23 is (73.04, 84.414), respectively. The results revealed a remarkable increase of Nusselt number by 55.89% for the pipe with twisted tape insert when compared to the horizontal pipe heat exchanger, implying that a heat exchanger with typical twisted tape is more efficient than a horizontal tube (HE). This behavior is due to the fluid in axial flow in the straight pipe. But with twisted tape, the swirl improves the recirculation flows between the walls and the center of the tube. In other words, at a specific distance from tube length, the fluid traverses a longer direction. Additionally, the created secondary flow causes the augmentation of the heat transfer rate. This increase in Nusselt number is more significant in higher Reynolds numbers.

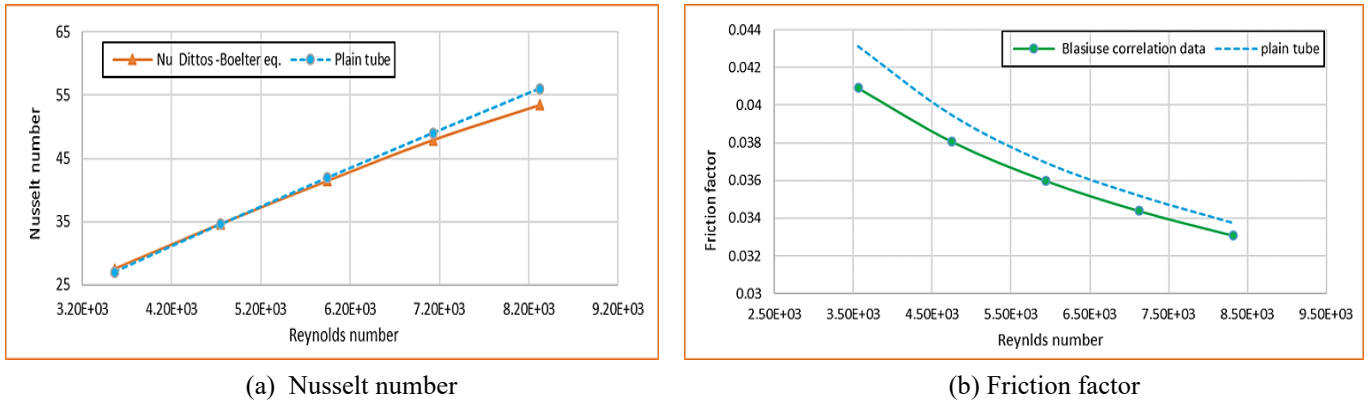


Figure 7: The effect of Reynolds number on the Nusselt number with Dittus –Bolter equation and friction factor with Blasius equation for distilled water

### 5.3 Twisted Tape and Hybrid Nanofluid Thermal Effect

As illustrated in Figure (9), the simulated data is translated into data of heat transfer coefficient, which are then converted into values of Nu along the pipe. The values of Nu are high at 1.8% volume fraction in the fully developed area, as can be seen in this diagram. Because of the stoppage in the fluid flow and the twisted tape's effect on the thermal boundary layer thickness, the Nu number increases in the presence of twisted tape. Figure (10) displays the change in average Nu with Reynolds number for a pipe with typical twisted tape. For all Reynolds number ranges, it is shown that as the Reynolds number rises, the average Nu number raises as well. For example, at a 1.8% volume fraction, the data shows a 30% increase in the Nusselt number.

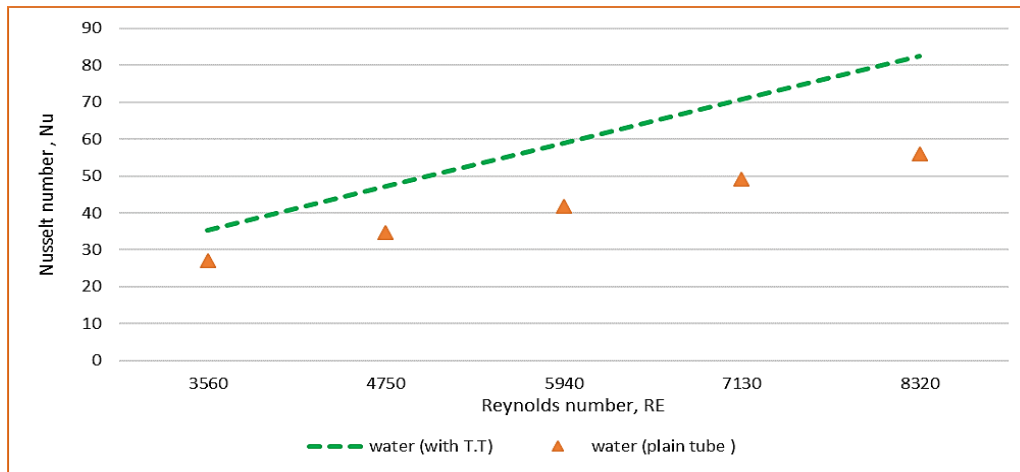


Figure 8: The numerical comparison between (with and without T.T) and Nusselt number

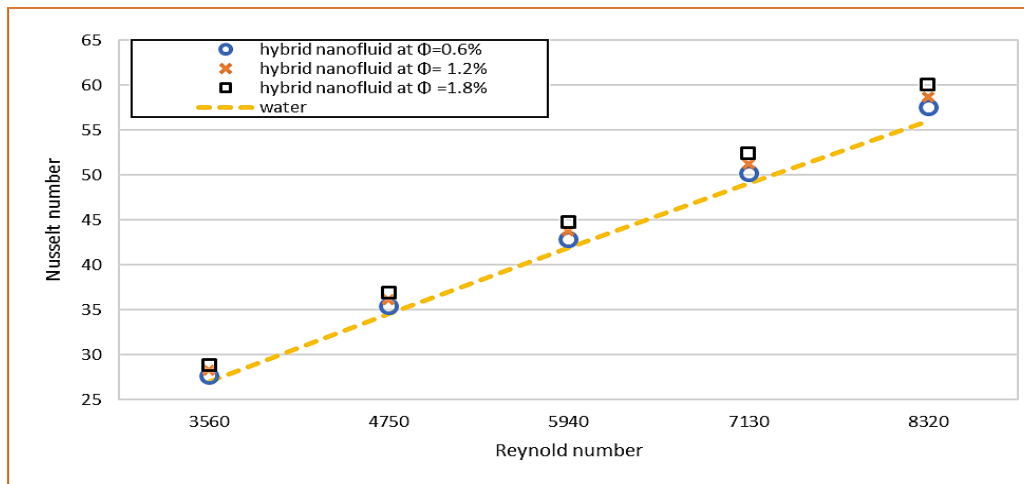


Figure 9: The effect of hybrid nanofluid volume concentration on the Nu at various Reynolds numbers

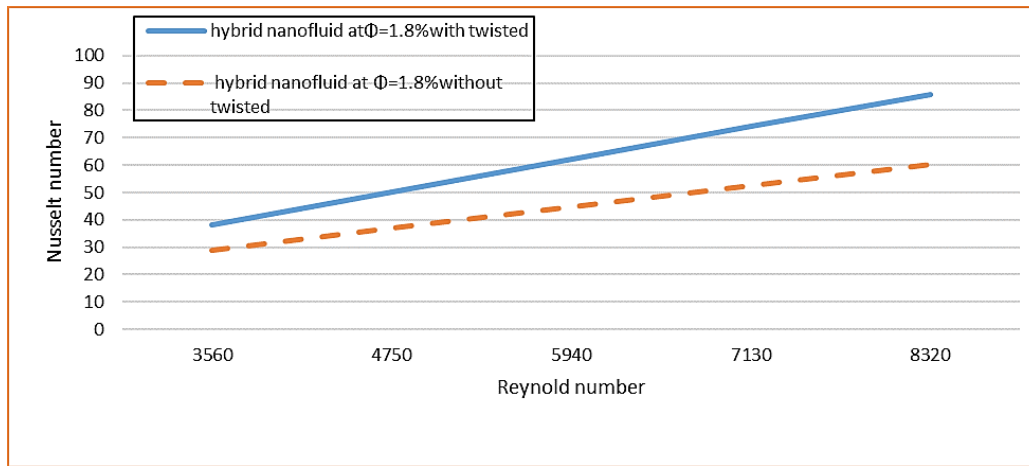


Figure 10: Effect of hybrid nanofluid at Φ=1.8% (with and without T.T) on the Nusselt number at different Reynolds numbers

### 5.4 Hydro-Dynamic Effect of Typical Twisted Tape with Hybrid Nanofluid

The pressure loss for the typical twisted tape in a hydro-dynamic flow through a horizontal circular pipe was computed numerically to evaluate the flow characteristics for the pipe with typical twisted tape at twist ratio (TR=9). The change of friction factor with the Reynolds number is seen in Figure (11). The friction factor tends to decrease as the Reynolds number increases, according to the simulation results. For the whole range of Reynolds numbers, the friction factor decreases as the Reynolds number increases because adding nanoparticles to water modifies the thermos-physical properties that significantly intensify the heat transfer rate inside the heat exchangers tubes. The other physical reason for the heat transfer augmentation is the Brownian motions of nanoparticles. The friction factor rises with increasing the volume fraction value in all situations with a hybrid nanofluid and at the same Reynolds number.

### 5.5 Pressure Drop

To fully understand the industrial uses of hybrid nanofluids, the pressure drop should be studied with the Nusselt number. Experiments on pressure loss as a function of Reynolds number are viewed in Figure 12. The Darcy friction factor may be computed with the following formula [21, 22]:

Where,  $\Delta p = p_{in} - p_{out}$

$$f = \frac{\Delta p}{L} \frac{D_h}{\rho V^2} \tag{17}$$

The pressure drop increased due to the increase in Reynolds number.

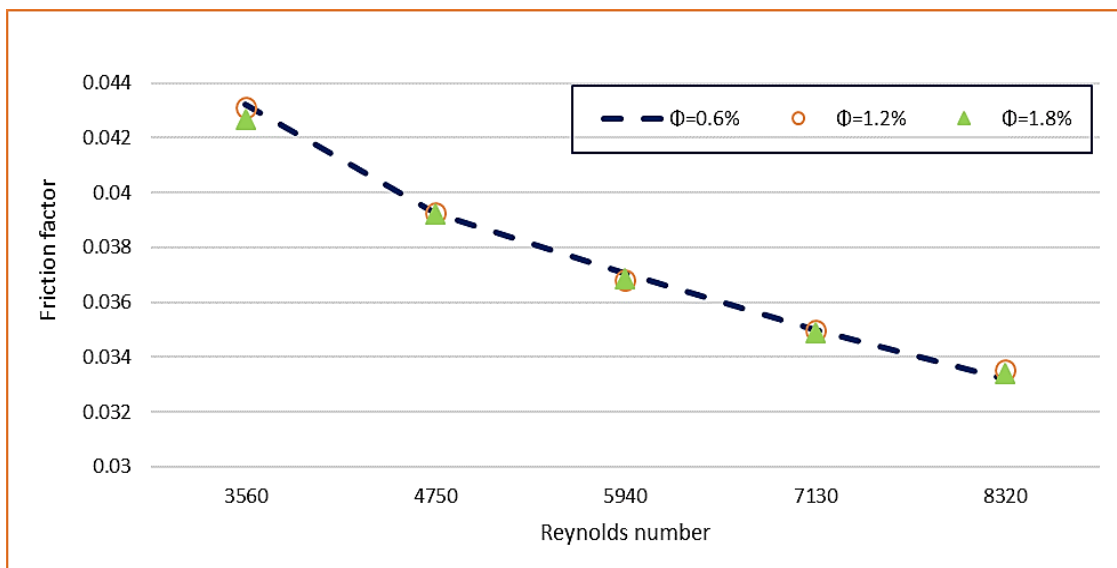


Figure 11: The effect of hybrid nanofluid with twisted tape on the friction factor number at different Reynolds numbers

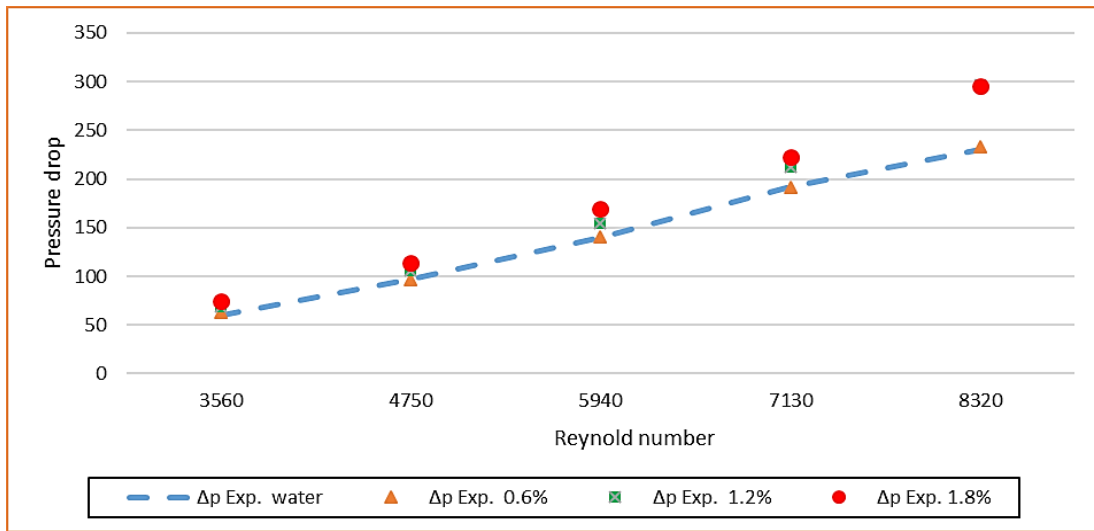


Figure 12: The effect of hybrid nanofluid on the pressure drop (experimental) at different Reynolds numbers

### 5.6 Thermal Performance Factor (TPF)

A higher thermal performance factor indicates the effect of the increased heat transfers because the device modification outweighs the effect of increased friction and vice versa. The equation proposed by Eiamsa-ard et al. [13] to estimate the heat transfer efficiency improvement mechanism. For the following equation (18)

$$\begin{aligned}
 \text{Case 1/T. P. F} &= \frac{\frac{Nu \text{ hybrid nanofluid}}{Nu \text{ water}}}{\left(\frac{fr \text{ hybrid nanofluid}}{fr \text{ water}}\right)^{1/3}} \\
 \text{Case 2 /T. P. F} &= \frac{\frac{Nu \text{ (hybrid nanofluid) with TT}}{Nu \text{ (hybrid nanofluid) plain tube}}}{\left(\frac{fr \text{ (hybrid nanofluid) with TT}}{fr \text{ (hybrid nanofluid) plain tube}}\right)^{1/3}} \tag{18}
 \end{aligned}$$

The change in thermal performance factor with Reynolds number is seen in Figure 13. The maximum PEC for the typical conventional tape is (2.05) at Reynolds number (8320), with (Φ = 1.8%) in the turbulent flow domain, according to this diagram.

### 5.7 Isothermal Contours

Figure (14) demonstrates the isothermal contours of variation temperature through the hybrid nanofluids along the tube length. And, Figure (15) shows the static temperature profile along the examined portion in the middle plane for a hybrid nanofluid with Φ= 1.8% and Re= 8320.

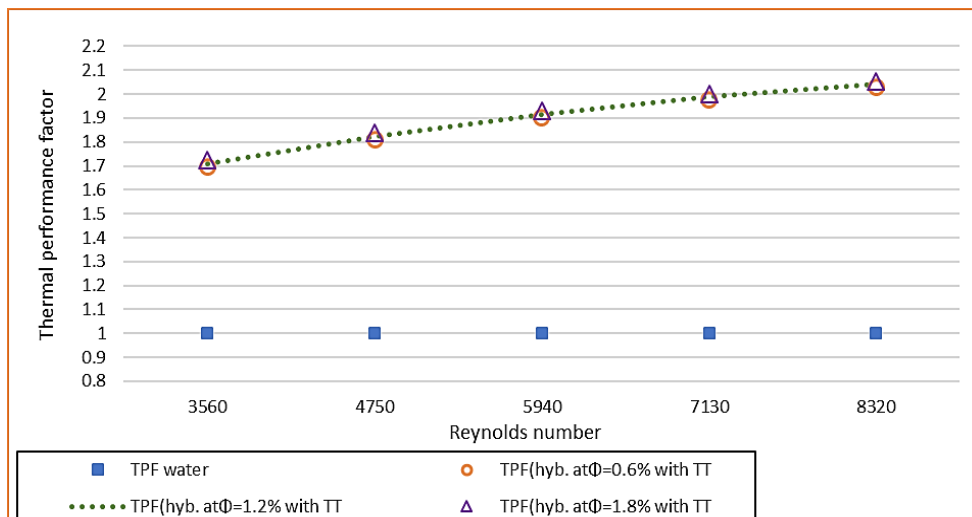


Figure 13: TPF for the hybrid nanofluid with typical twisted tape

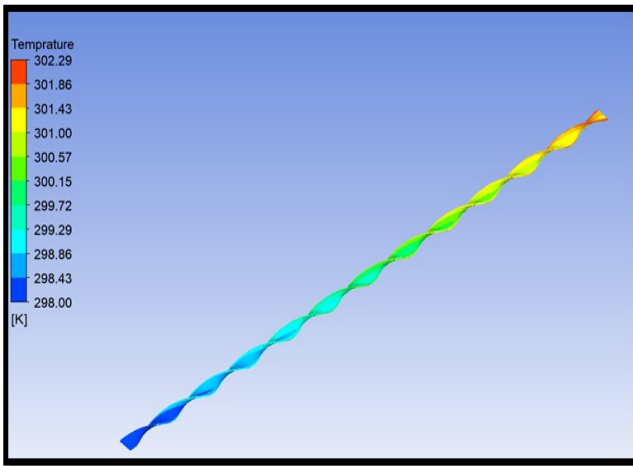


Figure 14: Temperature distribution along the examined portion for hybrid nanofluid ( $\phi=1.8\%$ )

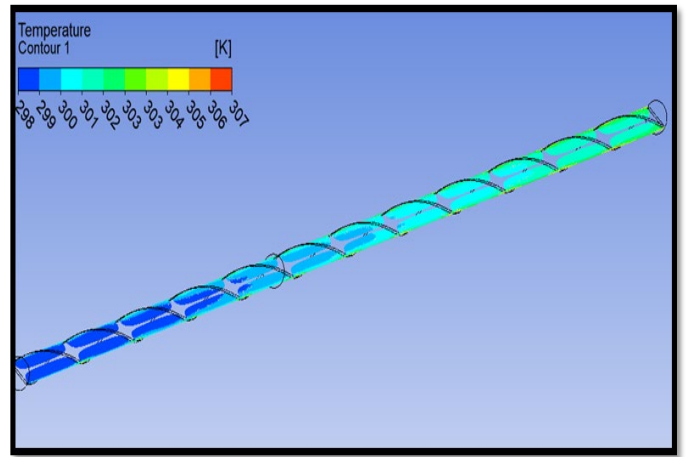


Figure 15: Static temperature contours for water at  $Re = 8320$

### 5.8 Pressure Contours

The pressure loss distribution contours for the horizontal pipe with a typically twisted tape insert and varied axial distance along the examined portion are shown in Figures (16) and (17). The pressure loss for the hybrid nanofluid passing through the pipe fitted with typical twisted tape is larger than the pressure loss for the pure water instances, as can be seen in these figures. Furthermore, when the volumetric flow rate raises, the pressure drop increases.

### 5.9 Velocity Contours

Figures (18) and (19) depict the velocity contours for a hybrid nanofluid with a volume fraction of 1.2 percent ( $Re = 3560$ ) and distilled water with the same Reynolds number along the test section ( $Z = 0$ , and 2 m), respectively.

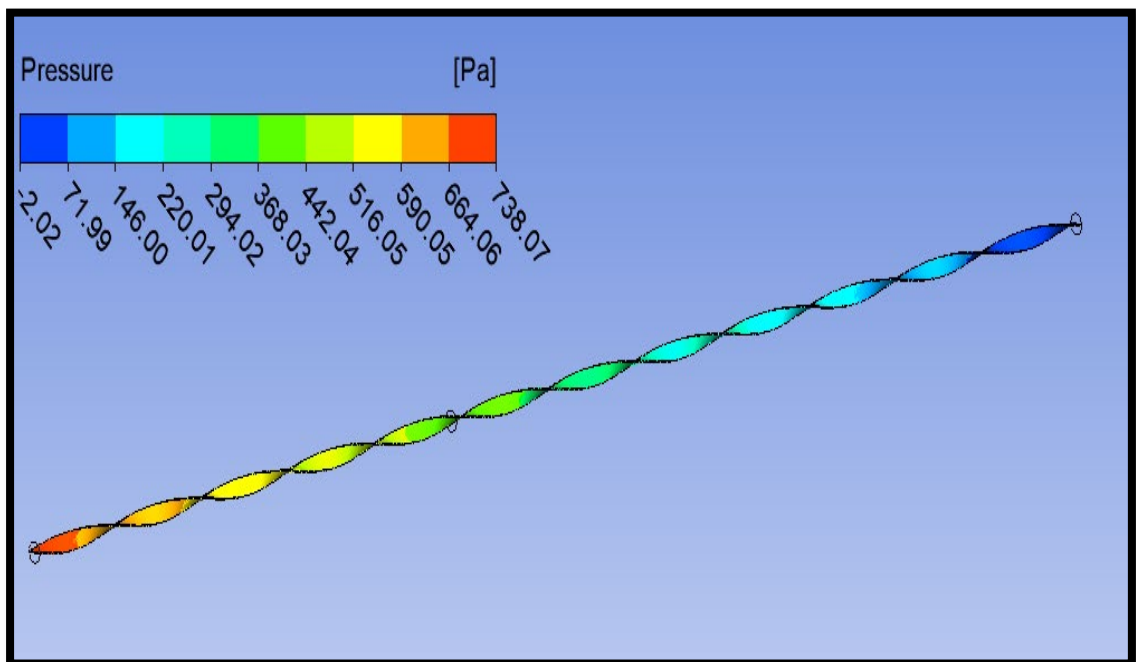


Figure 16: Pressure contours for the hybrid nanofluid ( $\phi=1.8\%$ ) and ( $Re=8320$ ) along the tube

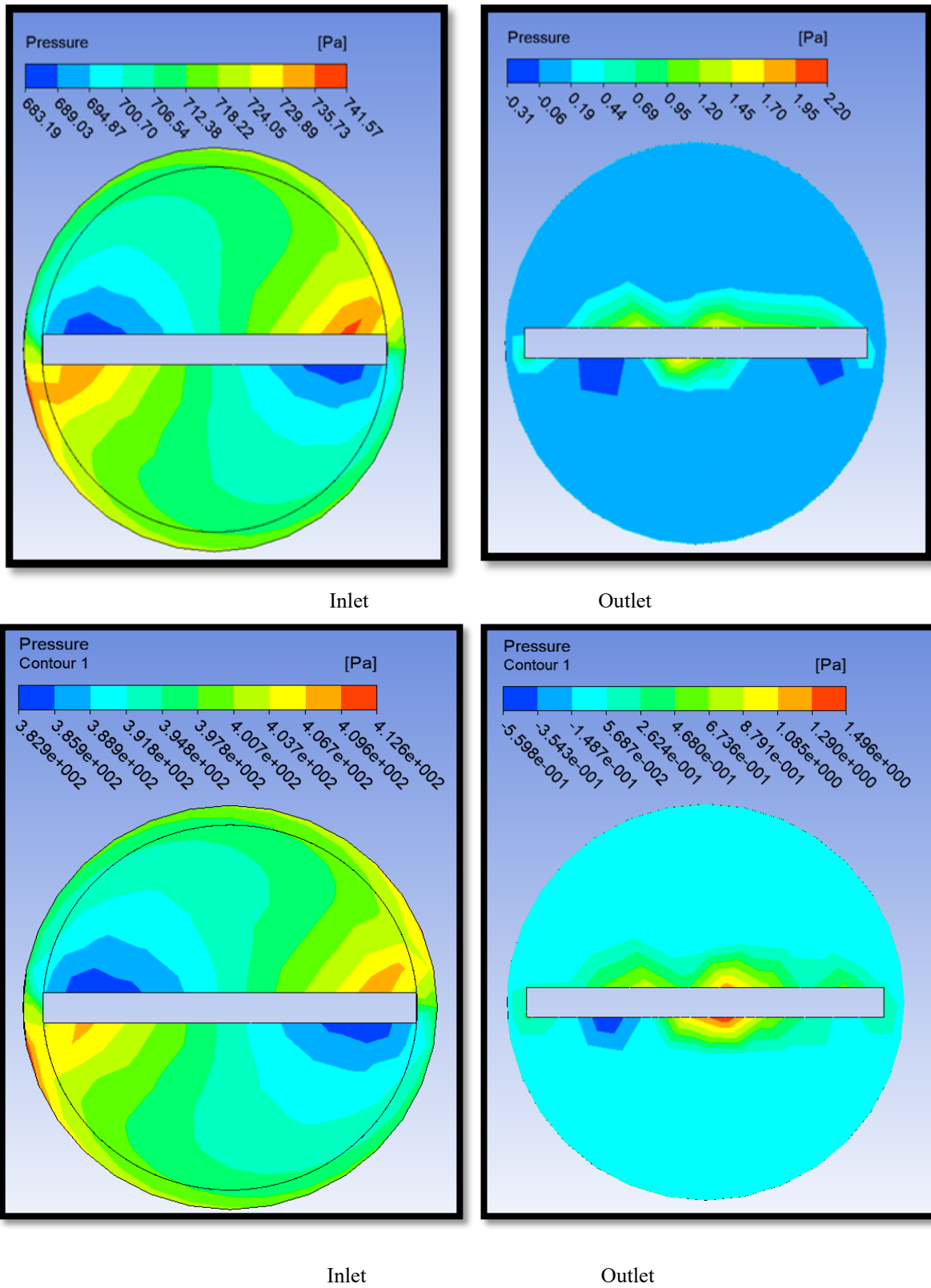


Figure 17: a. Pressure contours for the hybrid nanofluid ( $\phi=1.8\%$ ) and ( $Re=8320$ ), b. Pressure contours for the distilled water at ( $Re=5940$ )

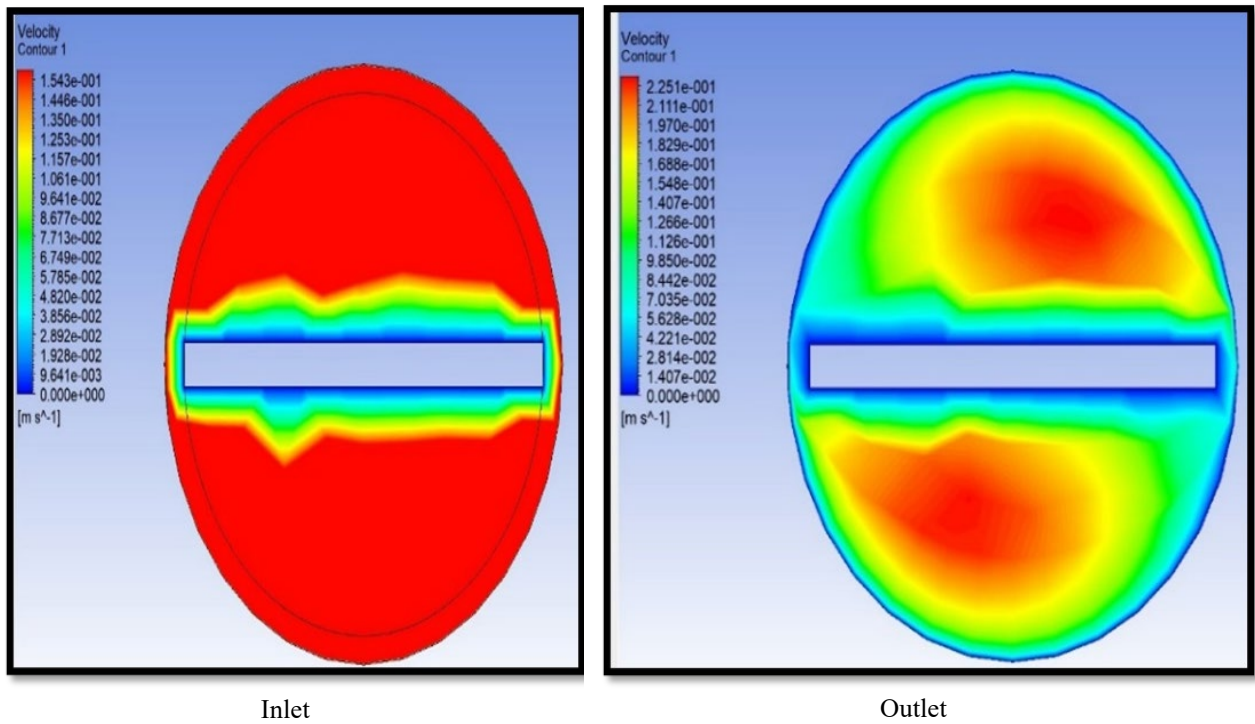


Figure 18: Velocity contours for the hybrid nanofluid ( $\phi=1.2\%$ ) and ( $Re = 3560$ )

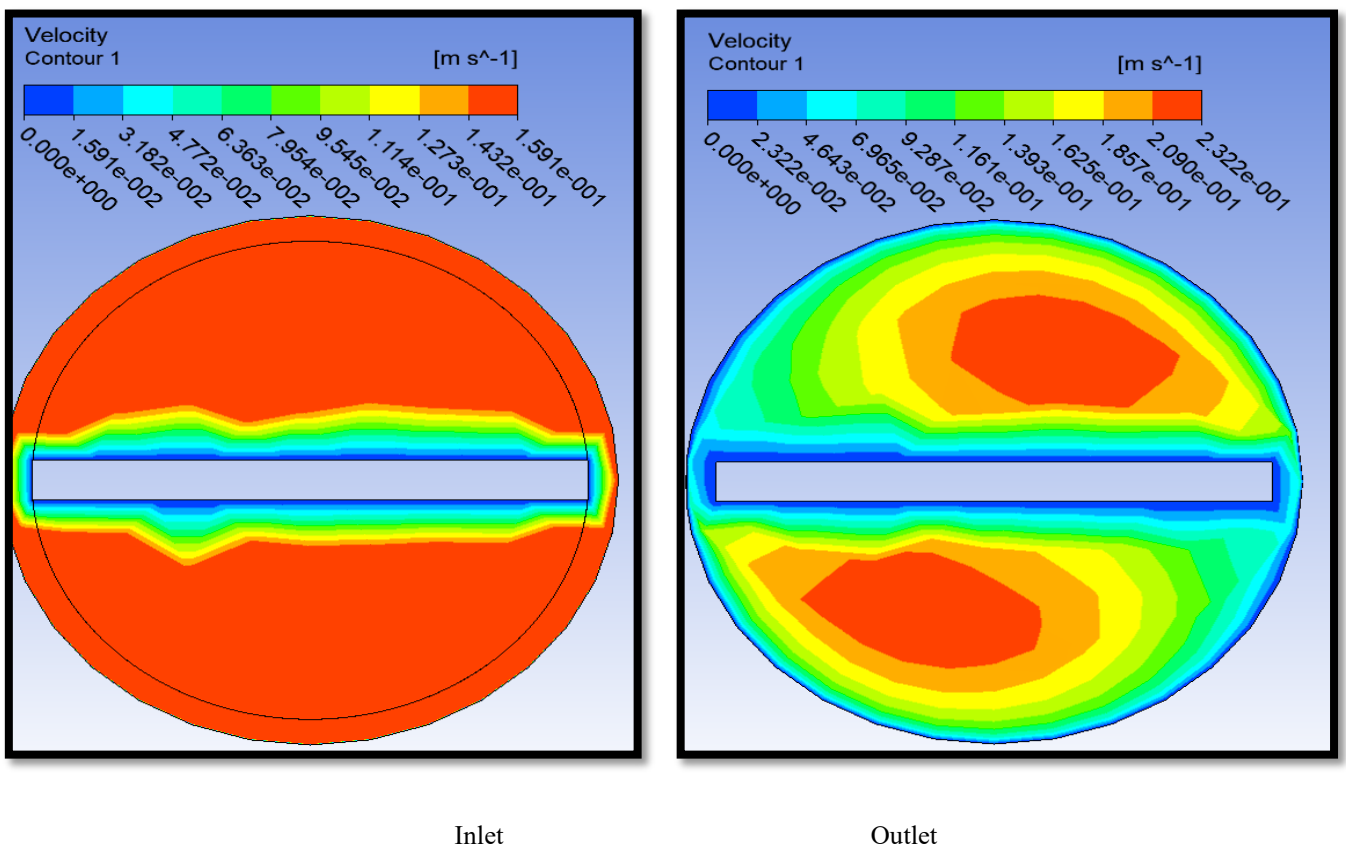


Figure 19: Velocity contours for water at ( $Re = 3560$ )

## 6. Conclusions

The hybrid nanofluid enhanced the heat transfer compared with the base fluid (distilled water) under the same Reynolds number, with a little increase of pressure drop, the heat transfer enhanced with increasing nanoparticles concentration, and ( $\phi=1.8\%$ ) gives higher heat transfer enhancement among the studied concentration. The combined use of the hybrid nanofluid

and twisted tape gives higher heat transfer enhancement compared to the individual use of each one. For all volume concentrations, the ratio raises as the Reynolds number rises. The average ratio rises approximately by about 0.292 with 0.6% volume concentration, increased by about 0.342 with 1.2% volume concentration, and raised by about 0.355 with 1.8% volume concentration, according to the findings.

The high Nu was obtained with the concentration of (1.8%) with an enhancement in the heat transfer (Nusselt number) about (6.70%) than water.

In Ansys-Fluent, using the finite volume method with a single-phase model provides numerical results that are typically in excellent agreement with experimental data, with both hybrid nanofluid and twisted tape within the tube; it is beneficial in predicting the pipe flow.

## Nomenclature

Greek Symbols		
SYMBOL	DESCRIPTION	UNITS
$\phi$	Volume fraction	-
$\rho$	Density	kg/m <sup>3</sup>
(TPF)	Thermal performance factor	-
$f$	Friction factor	-
$\mu$	Dynamic viscosity	kg/m.s

Subscripts	
Symbol	Description
$n_f$	Nanofluid
$h_{nf}$	Hybrid nanofluid
$k_{p1}, k_{p2}$	Thermal conductivity for particles 1 and 2, respectively
$k_{bf}$	Thermal conductivity for base fluid

## NOMENCLATURE

SYMBOL	Q	UNITS
CuO	Copper oxide	-
Al <sub>2</sub> O <sub>3</sub>	Aluminum oxide	-
PLA	(polylactic acid)	
T.T	Typical twisted tape	
CNTs	Carbon nanotubes	-
Fe <sub>3</sub> O <sub>4</sub>	iron(III) oxide	-
MWCNT	Multi-walled carbon nanotubes	-
TiO <sub>2</sub>	Titanium dioxide	-
CC-QTs	Quadruple counter tapes in cross directions	-
h	Heat transfer coefficient	W/m <sup>2</sup> .K
k	Thermal conductivity	W/m.K
Nu.	Nusselt number	-
p	Pressure	N/m <sup>2</sup>
TR	Twist ratio	-
Pr.	Prandtl number	-
Re.	Reynolds number	-
HE	Heat exchanger	
Di	Diameter	m
PEC	Thermal performance factor	-

## Author contribution

All authors contributed equally to this work.

## Funding

This research received no external funding

## Data availability statement

The data that support the findings of this study are available on request from the corresponding author.

## Conflicts of interest

Authors declare that their present work has no conflict of interest with other published works.

## References

- [1] E. Smithberg, F. Landis, Friction and Forced Convection Heat-Transfer Characteristics in Tubes With Twisted Tape Swirl Generators, *J. Heat Transfer*, 86 (1964) 39–48. <https://doi.org/10.1115/1.3687060>
- [2] S. W. Hong, A. E. Bergles, Augmentation of Laminar Flow Heat Transfer in Tubes by Means of Twisted-Tape Inserts, *J. Heat Transfer*, 98 (1976) 251–256. <https://doi.org/10.1115/1.3450527>
- [3] R. M. Manglik, A. E. Bergles, Heat Transfer and Pressure Drop Correlations for Twisted-Tape Inserts in Isothermal Tubes: Part II—Transition and Turbulent Flows, *J. Heat Transfer*, 115 (1993) 890–896. <https://doi.org/10.1115/1.2911384>
- [4] N.A. Sheikh, D.L.C. Ching, I. Khan, A Comprehensive review on theoretical aspects of nanofluids: Exact solutions and analysis, *Symmetry*, 12 (2020) 725. <https://doi.org/10.3390/sym12050725>
- [5] M. Dadhich, O. S. Prajapati, V. Sharma, Investigation of boiling heat transfer of titania nanofluid flowing through horizontal tube and optimization of results utilizing the desirability function approach, *Powder Technol.*, 378 (2021) 104–123. <https://doi.org/10.1016/j.powtec.2020.09.077>
- [6] S. U. S. Choi, Enhancing thermal conductivity of fluids with nano-particles, *ASME, FED*, 231(1995) 99–105. <https://ci.nii.ac.jp/naid/80008813348>
- [7] M. S. Tahat, A. C. Benim, Experimental Analysis on Thermophysical Properties of Al<sub>2</sub>O<sub>3</sub>/CuO Hybrid Nano Fluid with its Effects on Flat Plate Solar Collector, *Defect Diffus. Forum.*, 374 (2017) 148-156. <https://doi.org/10.4028/www.scientific.net/DDF.374.148>
- [8] M. N. Labib, M. J. Nine, H. Afrianto, H. Chung, H. Jeong, Numerical investigation on effect of base fluids and hybrid nanofluid in forced convective heat transfer, *Int. J. Therm. Sci.*, 71 (2013) 163-171. <https://doi.org/10.1016/j.ijthermalsci.2013.04.003>
- [9] L. S. Sundar, M. K. Singh, and A. Sousa, Enhanced heat transfer and friction factor of MWCNT–Fe<sub>3</sub>O<sub>4</sub>/water hybrid nanofluids, *Int. Comm. Heat Mass Transfer*, 52 (2014) 73–83. <https://doi.org/10.1016/j.icheatmasstransfer.2014.01.012>
- [10] S. M. Abbasi, A. Rashidi, A. Nemati, K. Arzani, The effect of functionalization method on the stability and the thermal conductivity of nanofluid hybrids of carbon nanotubes/gamma alumina, *Ceram. Int.*, 39 (2013) 3885–3891. <https://doi.org/10.1016/j.ceramint.2012.10.232>
- [11] S. Mosayebidorcheh, M. Sheikholeslami, M. Hatami, D. D. Ganji, Analysis of turbulent MHD Couette nanofluid flow and heat transfer using hybrid DTM–FDM, *Particuology*, 26 (2016) 95-101. <https://doi.org/10.1016/j.partic.2016.01.002>
- [12] H. Maddah, R. Aghayari, M. Farokhi, S. Jahanizadeh, K. Ashtary, Effect of Twisted-Tape Turbulators and Nanofluid on Heat Transfer in a Double Pipe Heat Exchange, *J. Eng.*, (2014) 9. <https://doi.org/10.1155/2014/920970>
- [13] S. Eiamsa-ard, K. Kiatkittipong, Heat transfer enhancement by multiple twisted tape inserts and tio<sub>2</sub>/water nanofluid, *Appl. Therm. Eng.*, 70 (2014) 896-924. <https://doi.org/10.1016/j.applthermaleng.2014.05.062>
- [14] K. Ghachem, W. Aich, L. Kolsi, Computational analysis of hybrid nanofluid enhanced heat transfer in cross flow micro heat exchanger with rectangular wavy channels, *Case Stud. Therm. Eng.*, 24 (2021) 100822. <https://doi.org/10.1016/j.csite.2020.100822>
- [15] I. Alesbe, S. H. Ibrahim, S. Aljabair, Mixed convection heat transfer in multi-Lid-driven trapezoidal annulus filled with hybrid nanofluid, *J. Phys. Conf. Ser.*, 1973 (2021) 012065. <https://doi.org/10.1088/1742-6596/1973/1/012065>
- [16] S. Aljabair, A. A. Mohammed, I. Alesbe, Natural convection heat transfer in corrugated annuli with H<sub>2</sub>O–Al<sub>2</sub>O<sub>3</sub> nanofluid, *Heliyon.*, 6 (2020). <https://doi.org/10.1016/j.heliyon.2020.e05568>

- [17] A. A.Karalah, N.S. Mahmoud, Experimental Investigation of Heat Transfer Enhancement with Nanofluid and Twisted Tape Inserts in a Circular Tube, *Eng. Technol. J.*, 34 (2016) 664-684.
- [18] R. J. Moffat, Describing the uncertainties in experimental results, *Exp. Therm. Fluid Sci.*, 1 (1988) 3-17. [https://doi.org/10.1016/0894-1777\(88\)90043-X](https://doi.org/10.1016/0894-1777(88)90043-X)
- [19] A. E. Bergles, Technique to augment heat transfer. In *Handbook of heat transfer Applications*, (Edited by Werren M. Rohsenow, James P. Hartnett, and Ejup N. Ganic), Ch. 3, 2nd Edition, McGraw-Hill Book company, NY.
- [20] J. P. Holman, *Heat Transfer*, 10th Edition, McGraw-Hill Companies, Inc., 2010.
- [21] F. M. White, *Fluid Mechanics*, 4th edition, McGraw-Hill books, 2001.
- [22] A. Behnampour, O. A. Akbari, M. R. Safaei, M. Ghavami, A. Marzban, A. S. Shabani, M. Zarringhalam, R. Mashayekhi, Analysis of heat transfer and nanofluid fluid flow in microchannels with trapezoidal, rectangular and triangular shaped ribs, *Physica E Low Dimens. Syst. Nanostruct.*, 91 (2017)15–31. <https://doi.org/10.1016/j.physe.2017.04.006>